Research Square

Preprints are preliminary reports that have not undergone peer review.
They should not be considered conclusive, used to inform clinical practice,
or referenced by the media as validated information.

# Superfluid helium excitations under pressure

**Franz Demmel**
SIS Facility
**Ken H Andersen**
Institut Laue-Langevin
**Oleg Kirichek**
oleg.kirichek@stfc.ac.uk

SIS Facility

**Research Article**

**Keywords:**

**Posted Date:** November 13th, 2026

**DOI:** https://doi.org/10.21203/rs.3.rs-11536824/v1

**License:** This work is licensed under a Creative Commons Attribution 4.0 International License.
Read Full License

**Additional Declarations:** No competing interests reported.

# Superfluid helium excitations under pressure

F. Demmel,[1,*] K. H. Andersen,[2] and O. Kiricheck[1,†]

[1] *ISIS Facility, Rutherford Appleton Laboratory, Didcot, OX11 0QX, UK*
[2] *ILL, 71 avenue des Martyrs, 38042 Grenoble Cedex 9, France*

(Dated: October 27, 2026)

The superfluid $^4$He excitation spectrum is investigated through inelastic neutron scattering with increasing pressure. This high energy resolution experiment covers pressures from 0 bar up to 24 bars near the solidification limit of helium at a low temperature of T=0.04 K. The high energy resolution of the spectrometer allowed to follow precisely the energy shifts at the maxon energy in relation to the roton excitation energy. With increasing pressure the maxon energy increases and saturates at p=15 bars whereas the roton energy continuously decreases with increasing pressure. The analysis demonstrates that the maxon energy will not exceed twice the roton energy. At p = 15 bar, we observe a marked increase in the interactions between the maxon elementary excitation and the multi-excitation spectrum. This enhanced coupling manifests itself directly in the reduced lifetime of the maxon, which serves as a clear signature of stronger scattering processes between the elementary excitations of superfluid helium and the continuum of multi-excitation states. Given the central role of liquid $^4$He as a model quantum fluid, these findings provide valuable insight not only into the microscopic dynamics of maxons but also into the broader mechanisms governing interactions among bosonic excitations. As such, the results contribute to a more general understanding of quasiparticle coupling and decay processes in strongly interacting Bose systems.

## I. INTRODUCTION

The Helium isotopes do not freeze when cooled down to temperature zero at atmospheric pressure. This is due to their weak interaction potential and the large zero point motion. The large de Broglie wavelength of the helium atom leads to a strong influence of quantum dynamics in this system. $^4$He is a boson and the statistics of the liquid is governed by the Bose Einstein statistics, a requirement to call $^4$He a quantum liquid [1]. At a pressure above 25 bar $^4$He solidifies into a bcc or hcp phase [2]. Liquid $^4$He undergoes a phase transition at T=2.17 K from a normal liquid to the superfluid phase, where the heat capacity shows a $\lambda$-like change, coining this phase transition the $\lambda$-transition. The superfluid phase is characterized by a non-viscous flow. A two-liquid hydrodynamic model was developed to describe the superfluid properties. The amount of the superfluid phase approaches 100% towards zero temperature. As a bosonic quantum liquid the expectation is that $^4$He will form a Bose-Einstein-Condensate (BEC). However, the dense superfluid helium is a strongly correlated system of bosons, where only a small fraction of the atoms are in the Bose condensate. This fact is in contrast to the noninteracting diluted alkali Bose gases [1]. In $^4$He the fraction of atoms in the BEC is about 10%, which was confirmed by path integral Monte Carlo simulations [3] and neutron scattering [4–6]. That surprising contrast between the large superfluid fraction and the small fraction of atoms in the condensate is related to the interplay of Bose condensation and the strong correlations in the dense liquid.

From the beginning a lot of effort was devoted to investigate the elementary excitations in the superfluid state. Landau introduced the concept of elementary excitations to provide a microscopic theory for the two-fluid hydrodynamics of superfluid helium [7]. The empirical dispersion relation of these excitations was derived from thermodynamic data and he introduced the *roton* term for the excitation at the minimum of the dispersion.

The elementary excitations consist of a continuous phonon-roton dispersion curve: a linear phonon part at low wave vectors followed by a maximum energy (called the maxon) and then a pronounced minimum excitation energy (called the roton). No further excitations with lower energy exist. Feynman and Cohen were able to derive an expression for the dispersion around the roton, which is related to the structure factor and hence the minimum in energy occurs around 2 $\mathring{A}^{-1}$ [8, 9]:

$$E(Q) = \frac{\hbar^2 Q^2}{2mS(Q)} \tag{1}$$

Feynman gave a pictorial explanation for the roton excitation with a circular backflow movement of atoms. Further on, considerable effort has been devoted to the development of an accurate theoretical description of the dynamics of superfluid $^4$He using various techniques [10–15]. The knowledge of the dispersion relation allows the calculation of low temperature thermodynamic properties of superfluid $^4$He [16]. The excitations considered by Landau, Feynman and others correspond to the single-particle response function associated with the description of an effective vacuum - the superfluid ground state [17] - and non-interacting quasiparticle excitations. The elementary excitations near T=0 are very long-living and hence the excitations are very sharp in energy, which is in stark contrast to excitations in classical liquids.

The instability of the elementary excitations against

* franz.demmel@stfc.ac.uk
† oleg.kirichek@stfc.ac.uk

decay into other elementary excitations in superfluid helium was studied theoretically by Pitaevskii [18]. He found that the excitation spectrum cannot exceed twice the roton energy. The consequence of this prediction is that at large wave vector the dispersion saturates at a value of twice the roton energy, which is not in agreement with the predicted dispersion of Feynman and Cohen, see Eq 1.

Neutron scattering is the most powerful tool to investigate excitations in superfluid helium and has been applied for nearly 70 years now, see for a recent review [19]. Neutron scattering gives access to the dynamic structure factor $S(Q,\omega)$, a quantity related to the dynamic susceptibility, i.e., the linear response of the system to a density fluctuation. Much of the early experimental work on superfluid $^4$He has focused on measuring the single-particle response function with a confirmation of the phonon-roton dispersion [20–24]. At wave vectors larger than 3.5 $\AA^{-1}$ the intensity of the excitation fades away and indeed a flattening of the dispersion was observed beyond the roton, although the energy seemed to exceed the two-roton energy. This puzzle was resolved through the combined theoretical and experimental work [25–30], and directly in a high-resolution neutron scattering experiment [31]. The spectrometer resolution allowed the separation of the sharp excitation peak, always located below the two-roton energy, from the high-energy continuum of excitations above the two-roton energy. That saturation behavior beyond the roton has been confirmed in an experiment at 20 bar pressure [32]. In experiments with broad resolution or performed at high temperatures, the two contributions are merged into a single peak, which appears to be above the two-roton energy, due to the asymmetry of the response [34–38]. Already in the first experiments additional intensity was observed at higher energies, above twice the roton energy [22]. These features are multi-excitations of the elementary quasi-particles. This part of the excitation spectrum is not included into the above mentioned theories about the elementary excitations. A theoretical description was devised to include the multi-excitation spectrum in addition to the elementary excitations and showed structure therein in energy and wave vector [39] and dynamic-many-body-theory was used to describe the multi-particle spectrum [15]. In addition, experimentally a ridge of intensity is observed near the helium atom recoil line [40]. In contrast to the elementary excitations these fluctuations are quite broad features in energy, see for example [22, 36, 40, 41].

With increasing pressure on the superfluid helium the maxon excitation energy will increase and the roton energy decrease. There might be a pressure when the maxon energy becomes larger than twice the roton energy with the consequence that the maxon would be allowed to decay. According to the conjecture from Pitaevskii this should not happen since the maxon would cease to exist as a well-defined elementary excitation.

The pressure dependence of superfluid helium was first studied in the seventies [23, 24]. These measurements, performed at T =1.1 K, revealed a crossing between the two modes. More recent pressure work with better resolution and statistics stopped at 20 bars [32, 42–46]. High-resolution measurements up to 24 bar showed again a crossing, but with a smaller magnitude [47]. These measurements, however, were performed at high temperatures, only 0.4 K below the $\lambda$- transition and the thermal broadening at such temperatures is expected to wash out the fine structure of the spectra. An observation of the maxon energy slightly exceeding the roton-roton decay threshold at p=24 bars was reported in [40]. More recently a pressure study at low temperature T=0.1 K was performed with a cold neutron time-of-flight spectrometer [48]. A precise analysis of the maxon and roton energy shifts were made for pressures up to p=10 bars and then p=24 bars with a best energy resolution of FWHM=0.07 meV combined with a very good wave vector resolution.

Here, we present high energy resolution neutron scattering experiments (FWHM=0.025 meV) to separate the maxon peak from the continuum of multi-excitations in superfluid $^4$He at a very low temperature of T=0.04 K with pressures ranging from 0 bar to 24 bars, near solidification. The energy resolution of the spectrometer is better than in the above mentioned experiment, however, with a coarser wave vector resolution. The roton energy is measured at the same time. These conditions allow to scrutinize the evolution of the elementary excitations with high precision against pressure without the deteriorating influence of temperature. Our analysis concludes that the maxon excitation does not cross the 2-roton energy, which would open up a decay mechanism. The maxon shows a maximum energy at about 15 bars and concomitantly the linewidth increases at this pressure, indicating interaction with the multi-excitation continuum. Our data [49] confirm the conjecture that the maximum energy of the elementary excitation dispersion in superfluid Helium remains below the 2-roton energy.

## II. EXPERIMENTAL DETAILS

High-purity $^4$He was condensed into a cylindrical Al-7075-T6 sample cell of 21 mm inner diameter and effective height of 50 mm and cooled to the base temperature of 40 mK. A novel nitrogen and helium free dry dilution refrigerator was used for this experiment [50]. Multiple scattering was reduced by 5 cadmium spacers of thickness 0.5 mm. The total sample volume was about 17 $cm^3$ and the molar volume of liquid helium at saturated vapor pressure below 1 K is 27.55 $cm^3$/mole. Condensation was done slowly, in order to keep the mixing chamber below 1 K, the still pressure not too high and in particular the condensing pressure from the compressor below 3 bars. Typical sample condensation rate was 0.05 bar-liters/min.

Neutron scattering measurements were performed at

the Osiris indirect time-of-flight backscattering spectrometer of the ISIS Facility, UK [51]. Osiris was operated in the PG002 high resolution mode and in the PG004 setting, offering extended Q coverage. The energy resolution is at the elastic line FWHM=0.025 meV at a final energy $E_f = 1.845\ meV$. The backscattering geometry results in a very high energy resolution in the inelastic region. Simulations predict a FWHM=0.027 meV at 1 meV energy transfer [52]. However, the small final energy restricts the available wave vector range to a maximum value of about $Q = 1.85\ \AA^{-1}$ at the elastic line, just not wide enough for the roton excitation, which is at $Q = 1.93\ \AA^{-1}$. Yet, the kinematics of the detector trajectories allows to measure the roton excitation with a maximum wave vector of $Q = 1.98\ \AA^{-1}$ at this energy transfer. With higher pressure the wave vector for the roton minimum position moves to larger wave vectors [48] and hence we are not able to measure the minimum energy completely within this instrument setting. To circumvent this limitation we performed additional measurements with the PG004 configuration. The final energy is $E_F = 7.38\ meV$ and the maximum wave vector is about $3.6\ \AA^{-1}$. The extended wave vector range comes with an increased energy resolution which is now FWHM=0.1 meV and a factor two increased Q-resolution. As a side effect this configuration has a factor 5 higher intensity.

Measurements of superfluid $^4$He were performed at a temperature of T=$40 \pm 4\ mK$ and pressures of 0, 5.0, 10.0, 15.0, 20.0, 22.2 and 24 bars. The empty sample cell was measured on cooling at temperatures between 1.5 and 0.05 K. Typical measurement times were 10-15 hours in the PG002 configuration and 2-4 hours in the PG004 mode.

Data analysis included a constant energy binning into $\Delta E = 0.002\ meV$ ($\Delta E = 0.005\ meV$) and constant Q-binning into $\Delta Q = \pm 0.025\ \AA^{-1}$ ($\Delta Q = \pm 0.05\ \AA^{-1}$) for the PG002 setting and the respective values for PG004 are given in brackets. The excitations, excluding the elastic line, were fitted with a single Lorentzian function convoluted with the zero energy transfer measured resolution function to derive the dispersion relations and the width of the excitations. The resolution function was obtained from a measurement with a vanadium standard and no adjustment was made for the use at the inelastic position. All maxon values were obtained from the high-resolution PG002 measurements at a fixed wave vector $Q = 1.12\AA^{-1}$. Due to the high energy resolution reliable values for the width and hence for the lifetime of the excitation could be obtained. The excitation energies at the roton minimum were derived from measurements with the PG004 setting to cover the whole minimum. Due to the coarse coverage with detectors in this wave vector range the minimum value was determined through a fit with a parabola in the wave vector range between $Q = 1.8\ \AA^{-1}$ and $2.2\ \AA^{-1}$. A parabola as an approximation for the dispersion around the roton minimum was already suggested by theory early on [7, 9]. All analysis steps have been performed within the Mantid software framework [53].

## III. RESULTS AND DISCUSSION

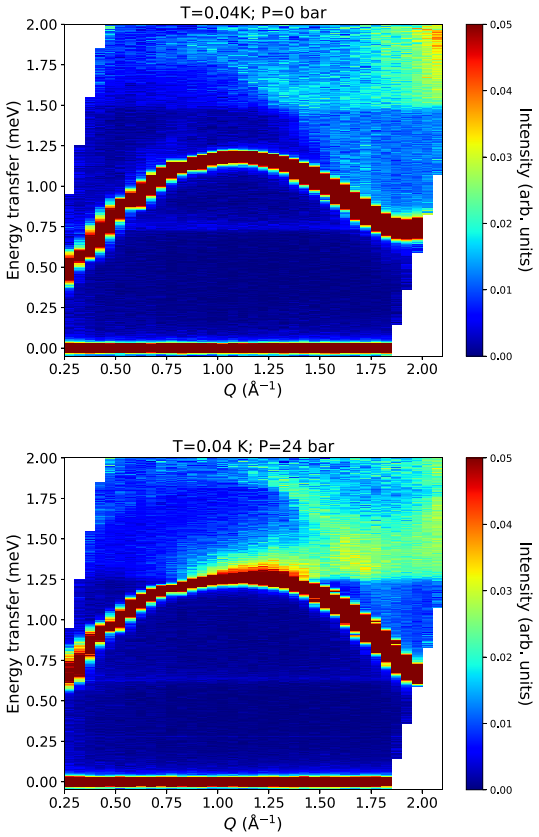



FIG. 1. Intensity maps are shown for 0 bar and 24 bar pressure measured with the PG002 configuration.

In figure 1 we present intensity color maps for 0 bar and 24 bar pressure in the PG002 setting. Clearly visible is the dispersion of the sharp phonon-roton excitation and separated the multi-excitation spectrum above twice the roton energy. The plot for 24 bar pressure demonstrates a wave vector shift of the roton minimum to a larger Q-vector and an energy shift of the maxon excitation towards the multi-phonon spectrum, whose edge is lowered. The plot also indicates that the multi-excitation spectrum has a complex structure, which is linked to the nature of their formation, pairs of rotons or maxons and their mixture[36, 40, 48]. However, we will not discuss the details of the multi-excitation spectrum furthermore.

Visible in the intensity map of the PG002 setting is a weak intensity at constant energy emerging from the roton excitation, which probably is due to a multiple scattering effect. Even though the multiple scattering is reduced due to the cadmium sheets inside the sample cell the roton excitation is strong enough that some

multiple scattering events can not be avoided. That the roton excitation is involved in this scattering event can be deduced from the high-pressure plot, where this constant energy line of intensity is shifted to lower energies accordingly. Note that at low Q-vectors this multiple scattering feature crosses the phonon excitations. In the plot with 0 bar pressure a sharp line at about 0.27 meV appears across all detectors, which is due to a glitch in the data acquisition electronics for this specific run.

Figure 2 shows the 0 bar result from the PG004 setting, now covering the whole roton excitation dispersion. This plot also depicts the wave vector range beyond the roton minimum, where the excitation intensity slowly dies out around $Q \approx 3.5$ Å$^{-1}$. The maximum energy of the elementary quasi-particle excitations saturates around 1.5 meV beyond the roton minimum, hence twice the roton energy. Some time ago it has been demonstrated that the elementary excitation in superfluid helium will not exceed twice the roton energy in this wave vector range [31]. Furthermore, an intensity ridge is visible at larger energy transfers, located at wave vectors larger than $Q \approx 2$ Å$^{-1}$. Included as a line is the free particle dispersion of a Helium atom. That line coincides at large wave vectors with this intensity distribution and points to the fact that the neutrons are scattered from an individual helium atom.

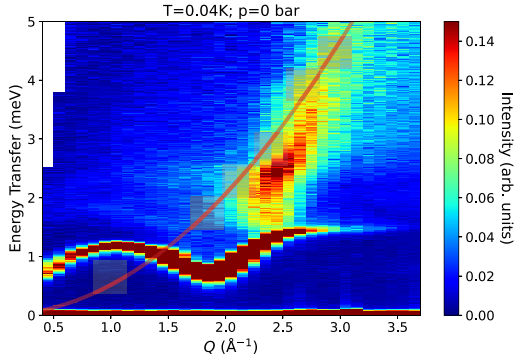



FIG. 2. The intensity map shows the excitation spectrum for a wide wave vector and energy range from the PG004 configuration at p=0 bar. Included is also the free particle dispersion for a Helium atom.

In figure 3 three spectra are plotted taken in the PG002 mode at 0 bar pressure. The three Q-vectors are in the phonon region ($Q = 0.33$ Å$^{-1}$), at the maxon ($Q = 1.12$ Å$^{-1}$) and at the roton (1.92 Å$^{-1}$). The excitation spectrum is clearly dominated by the huge intensity of the roton excitation. In contrast, the maxon excitation intensity and, in particular, the phonon mode intensity are much weaker. The inset shows an augmented view into the spectra, where now also the intensity of the multi-excitations becomes visible beyond 1.5 meV. Included is the empty can spectrum which is negligible small in the inelastic region. It shows some intensity around zero energy transfer, which probably enables the multiple scattering contribution.

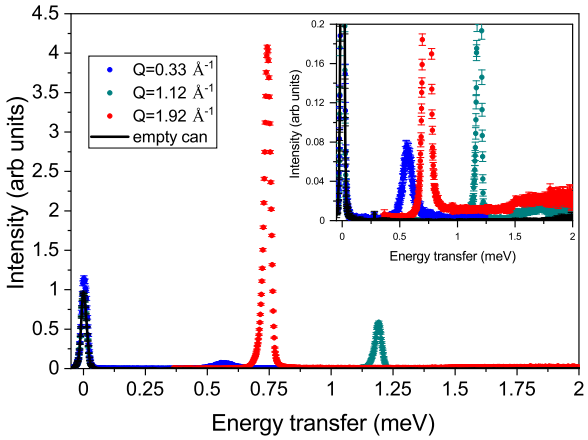



FIG. 3. Spectra of the 0 bar measurement with the PG002 setting are plotted for three Q-vectors. Included is the empty cell measurement. The inset shows an augmented view into the small intensity region.

In figure 4 spectra at the maxon position and the roton position are shown for 4 pressures. The maxon spectra in plot (a) are taken with the PG002 configuration and the roton spectra in plot (b) with the PG004 setting. The maxon energy shifts to higher energies with increasing pressure, where the largest shift already occurs with the pressure increase to p=10 bar. At the highest pressure the spectrum broadens and indicates a shift to lower energies. Also a high energy tail becomes visible from the multi-excitation spectrum. The roton mode shows a continuous reduction in energy with increasing pressure. The lines depict fits with a single Lorentzian lineshape convoluted with the respective resolution function. Most spectra are described reasonably well, however, the roton excitation at the highest pressure shows a deviation from a simple Lorentzian line shape.

Figure 5 depicts the fit results for the excitation energies. In panel (a) the excitation energies for 3 pressures (p=0 bar, p=10 bars and p=24 bars) are plotted for all wave vectors from fits to the PG002 spectra. In the small wave vector phonon region the energies are continuously increasing with higher pressure as expected. There seems to be a kink in the dispersion around $Q \approx 0.6$ Å$^{-1}$. That feature weakens with increasing pressure and is probably linked to a disturbance of the fit from the multiple scattering signal originating at the very strong roton peak (see figure 1). The line shape distortion at this wave vector leads to a shift in the position of the elementary excitation energy. For p=0 bar at $Q = 0.425$ Å$^{-1}$ we obtain a phase velocity of the phonon excitation of 250.4 m/s, which is in good agreement with literature values [48]. We will not discuss further the phonon wave vector range.

Panel (b) shows in detail the excitation energy changes in the maxon region for all measured pressures. At the

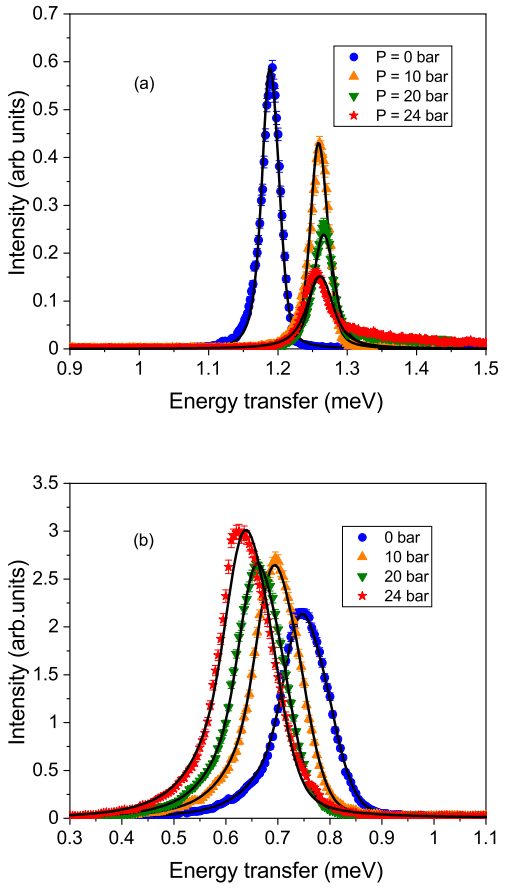



FIG. 4. Panel (a) shows spectra at the maxon (PG002) and panel (b) shows spectra at the roton (PG004) with a fit of the excitation (line) for 4 pressures: 0, 10, 20 and 24 bar.

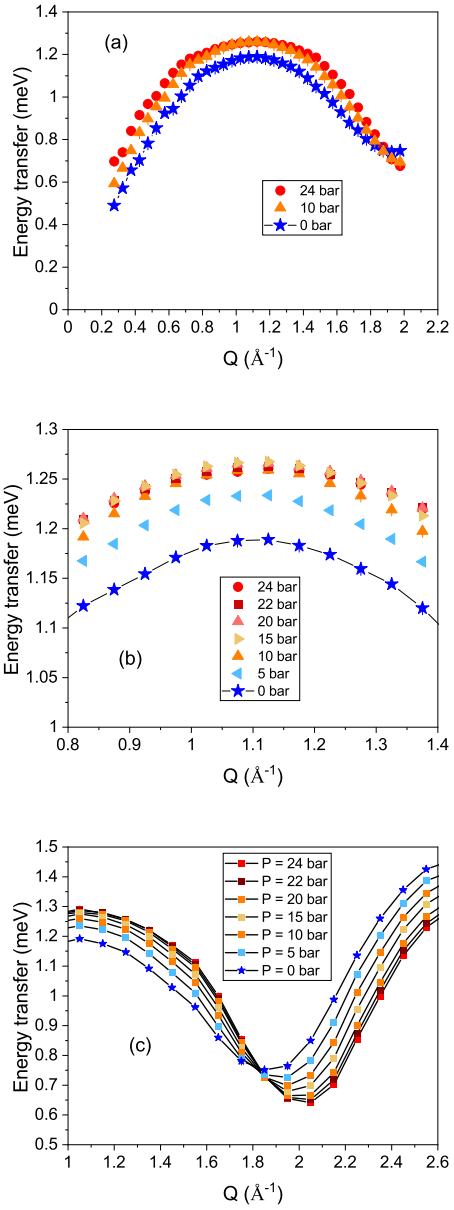



FIG. 5. The excitation energies are plotted against the wave vector are plotted in panel (a) for three pressures. Panel (b) shows the dispersion around the maxon and panel (c) around the roton excitation for all measured pressures.

maxon region there is a decisive shift to larger energies at p=10 bars and then only a small shift with p=24 bars within the symbol size. It seems the maximum excitation energy is reached at p=15 bars and at higher energies the dispersion is repelled. In panel (c) the roton energy region is plotted from the fits of the PG004 configuration. Clearly visible is the wave vector shift in the minimum position with rising pressure. The roton energy is continuously decreasing with rising pressure.

In table I we present the fit results for the excitation at the maxon wave vector. We applied a fit to the spectrum at $Q = 1.12$ Å$^{-1}$, which describes the lineshape well, see figure 4(a). These spectra were taken with the high-resolution configuration, which explains also the very small error bars in the energies. The $\Delta_{maxon}$ values are in excellent agreement with the most recent literature [48]. We take this excellent agreement as evidence for the quality of our data and data analysis. The values for the maxon energy show a maximum value at p=15 bars and then decrease slightly towards higher pressure.

In table II the energies at the roton minimum are provided. These were taken in the PG004 configuration with a 4 times worse energy resolution and a factor two worse Q-resolution. To determine the minimum Q-position a parabola fit to the dispersion was applied. The first row shows the result for p=0 bar from the PG002 measurement. Here the roton minimum is just covered by the configuration, see figure 4 (a). The obtained value $\Delta_{roton} = 0.7419 \pm 0.0002\ meV$ from a fit at $Q = 1.925$ Å$^{-1}$ agrees perfectly with the published value from Godfrin et al $\Delta_{roton} = 0.7418\ meV$ [48]. Due to the sparse detector coverage and the less good energy resolution the minimum wave vector position and roton energy

TABLE I. maxon energies

| p (bar) | $\Delta_{maxon}$ (meV) | $\Delta_{maxon}$ (meV) [48] |
|---|---|---|
| 0 | 1.187 ± 0.00006 | 1.19 ± 0.001 |
| 5 | 1.233 ± 0.00007 | 1.236 ± 0.001 |
| 10 | 1.259 ± 0.0001 | 1.26 ± 0.001 |
| 15 | 1.267 ± 0.0002 | |
| 20 | 1.266 ± 0.0006 | |
| 22 | 1.263 ± 0.0002 | |
| 24 | 1.260 ± 0.0002 | 1.263 ± 0.001 |

TABLE II. roton energies

| p (bar) | $Q_r$ ($\AA^{-1}$) | $\Delta_{roton}$ (meV) | $\Delta_{roton}$ (meV) [48] |
|---|---|---|---|
| 0 (PG002) | 1.925 ± 0.005 | 0.7419 ± 0.0002 | 0.7418 ± 0.001 |
| 0 (PG004) | 1.849 ± 0.005 | 0.748 ± 0.00493 | |
| 5 | 1.892 ± 0.005 | 0.724 ± 0.00543 | 0.7148 ± 0.001 |
| 10 | 1.935 ± 0.003 | 0.698 ± 0.00308 | 0.689 ± 0.001 |
| 15 | 1.960 ± 0.004 | 0.679 ± 0.00413 | |
| 20 | 1.984 ± 0.005 | 0.659 ± 0.00531 | |
| 22 | 1.998 ± 0.005 | 0.650 ± 0.00546 | |
| 24 | 2.006 ± 0.005 | 0.643 ± 0.0057 | 0.626 ± 0.001 |

are deviating in this configuration. At 0 bar pressure we obtain a shift in the minimum wavevector of $-0.07$ $\AA^{-1}$ and in energy a 0.006 meV larger roton energy. Previously, also slightly larger values for the roton energy were published [33, 36]. At p=24 bars we obtain a shift in the wavevector of $\Delta Q_r = -0.04$ $\AA^{-1}$ and in energy of 0.017 meV to a larger roton energy compared to [48].

In figure 6 the widths of the excitations are plotted for 0 and 24 bar pressure over all wave vectors in the PG002 configuration, which provides the highest resolution. Qualitatively the widths are very similar to a previous study [40]. In particular the strong increase of the width in the small Q phonon region is similar and the strong change in the maxon wave vector range with p=24 bar. In the small Q phonon region the width is increasing towards smaller wave vectors, which is related to the fact how the resolution ellipsoid cuts through the dispersive excitation. Within this wave vector range no quantitative conclusions can be drawn from this measurement without a sophisticated 4-dimensional resolution deconvolution. However, there is evidence that with pressure increase the width increases and hence the lifetime of the phonon modes decreases. At p=0 bar our widths are about a factor 5 smaller due to a better energy resolution compared to [40]. The most striking change with pressure occurs around the maxon excitation, where the above argument with the dispersive nature of the excitation is negligible. Here, the width increases by about a factor 5 with the pressure increase to 24 bar. In this wave vector range the lifetime of the excitation is probably reduced due to interactions with the multi-excitation spectrum. In figure 3 the spectrum at p=24 bars shows a high energy tail evidencing the influence from this interaction.

In figure 7 the excitation energies against the pressure are plotted. The energy of twice the roton excitation 2 $\Delta_{roton}$ (circles) is plotted together with the maxon energy (stars). The maxon energy shows a saturation behavior with a maximum value around p=15 bars, whereas the twice roton energy is continuously falling. However, even at the highest pressure, near solidification, the two values do not cross each other. A crossing is avoided due to the saturation-like behavior of the maxon energy.

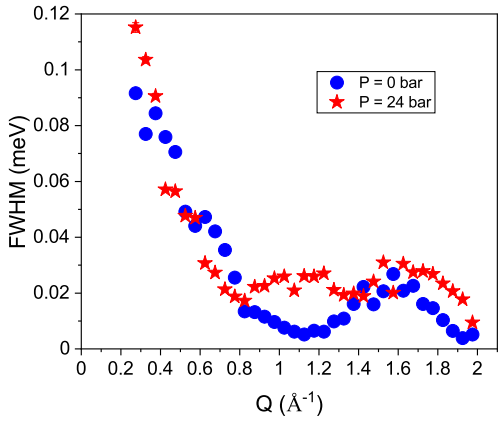



FIG. 6. The widths of the excitations are plotted for all wave vectors for p=0 bar and p=24 bar.

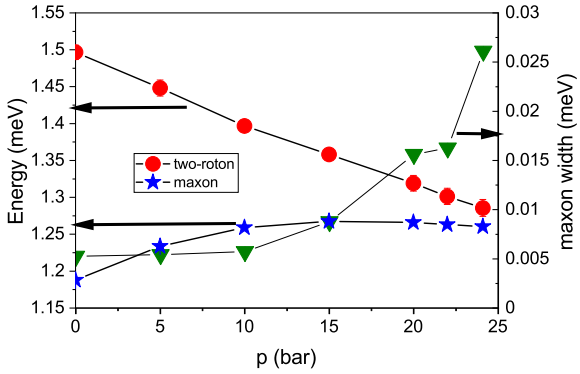



FIG. 7. The excitation energies for the 2-roton and the maxon are plotted against the pressure. Included is the linewidth of the maxon excitation with the scale on the right side.

Included in the plot is the width of the maxon excitations (triangles) with the scale on the right side. At low pressure the fit returns a width of FWHM=0.005 meV, which we assign to the increase in energy resolution when departing from zero energy transfer and hence to a practically zero width for the maxon excitation at this temperature. The lifetime of the excitation is longer than the spectrometer can resolve for $p < 10$ bar. However, at p=15 bar the width starts to increase and at the same time the excitation energy saturates.

In figure 8 the maxon excitation spectra are plotted for 4 pressures with an augmented view onto the multi-excitation spectrum development. At p=0 bar the multi-

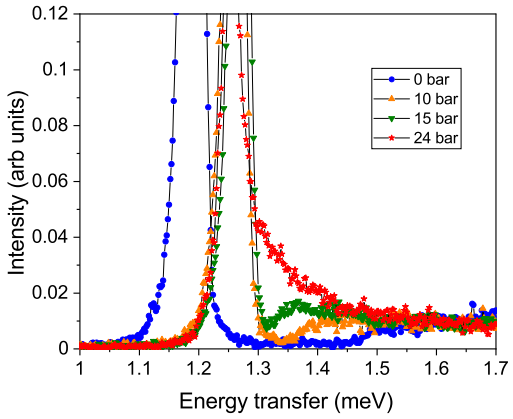



FIG. 8. Spectra at the maxon are plotted for 4 pressure values.

excitation spectrum is well separated from the sharp maxon. The gap is reduced at p=10 bar and then at p=15 bars both are approaching each other, evidencing an interaction between the elementary excitations and the multi-excitations. At p=24 bar the tail of the multi-excitation spectrum has reached the edge of the maxon excitation. The tail of multi-excitation intensity at p=24 bar agrees very well with a previous measurement [40]. It is conceivable that the elementary excitation interacts with the multi-excitation spectrum and consequently decay mechanisms open up, which lead to a reduction in lifetime and the maxon energy does not increase furthermore with pressure. With increasing temperature a decay process related to the number of thermally activated quasi-particles was observed [37] and could be described through the Landau-Kalathnikov damping mechanism. Here at nearly T=0 K a different type of damping process must be responsible. The interaction with the multi-excitation spectrum leads to a damping mechanism with a renormalization of the maxon energy and a decreasing lifetime of the excitation.

## IV. CONCLUSIONS

We performed an inelastic neutron scattering experiment to reveal the behavior of the superfluid excitations in $^4$He with increasing pressure. The experiment was undertaken with a cryogen-free dilution refrigerator at a record low temperature of T=0.04 K throughout the experiment. The high energy resolution not only allowed a precise determination of the excitation energies but also the change of the excitation lifetime with pressure could be revealed. The roton energy is continuously decreasing with increasing pressure whereas the energy of the maxon excitation shows a saturation at a pressure of p=15 bar. From our results we can conclude that the excitation energy of twice the roton and the maxon avoid a crossing in the whole pressure range and confirms the conjecture from Pitaevskii. The maxon excitation demonstrates a decrease in lifetime with increasing pressure above p=15 bar. Because the measurement was performed near T=0 K thermal effects can be excluded for this lifetime decrease. That achievement was possible due to the superb energy resolution of the spectrometer. Here we observe the interaction between the multi-excitation spectrum and the maxon excitation as they approach each other with increasing pressure. Their avoided crossing demonstrates clear mode-repulsion behavior. The presented experimental results could serve as input for novel theoretical studies on the complex dynamics of a highly correlated quantum liquid.

## V. ACKNOWLEDGEMENTS

Björn Fåk initiated this project and conducted this experiment in his very own excellent manner. Unfortunately he was not able to publish these wonderful results and we decided to publish the data *in memoriam*. We warmly thank Richard Down and his team of the ISIS Sample Environment Group for never giving up on the idea to perform this difficult experiment and all the efforts they put in to get the refrigerator working and Lev Melnykovskiy for fruitful discussions. This work was supported by the Science and Technology Facilities Council, STFC.

[1] A.J. Leggett, *Quantum liquids* (Oxford University Press, Oxford, 2010).
[2] H.R. Glyde *Excitations in liquid and solid Helium* Clarendon Press, Oxford (1994).
[3] D. M. Ceperley, Rev Mod Phys **67**, 279 (1995).
[4] V. F. Sears, E.C. Svensson, P. Martel, A.D.B. Woods, Phys. Rev. Lett. **49** 279 (1982).
[5] R.T. Azuah, W.G. Stirling, H. R. Glyde, M. Boninsegni, P. E. Sokol, S.M. Bennington, Phys. Rev. B **56**, 14 620 (1997).
[6] H. R. Glyde, R. T. Azuah, and W. G. Stirling, Phys. Rev. B **62** 14337 (2000).
[7] L. Landau, J. Phys. (USSR) **5**, 71 (1941).
[8] R. P. Feynman, Phys. Rev. **94**, 262 (1954).

[9] R. P. Feynman and M. Cohen, Phys. Rev. **102**, 1189 (1956); M. Cohen and R. P. Feynman, Phys. Rev. **107**, 13 (1957).

[10] N.N.Bogoliubov, Journal of Physics (USSR), **11**, 23–32 (1947).

[11] A. Zawadowski, J. Ruvalds, and J. Solana, Phys. Rev. A **5**, 399 (1972).

[12] A.K. Rajagopal and G. S. Grest, Phys. Rev. A **10**, 1837 (1974).

[13] K. Bedell, D. Pines, A. Zawadowski, Phys. Rev. B **29**, 102 (1984).

[14] C.E. Campbell and E. Krotschek, Phys. Rev. B **80**, 174501 (2009).

[15] C.E. Campbell, E. Krotschek, T. Lichtenegger Phys. Rev. B **91**, 184510 (2009).

[16] D. Pines and P. Nozieres, *The theory of quantum liquids* Vol. I (Addison-Wesley, 1990).

[17] H. Godfrin, M. Meschke, H.-J. Lauter, A. Sultan, H. M. Böhm, E. Krotscheck and M. Panholzer, Nature **483**, 576 (2012).

[18] L. P. Pitaevskii, Zh. Eksp. Theor. Fiz. **36**, 1168 (1959), [Sov. Phys. JETP **9**, 830 (1959)].

[19] H. R. Glyde, Rep. Prog. Phys. **81**, 014501 (2018)

[20] H. Palevsky, K. Otnes, and K. E. Larson, Phys. Rev. **108**, 1346 (1957); Phys. Rev. **112**, 11 (1958).

[21] J. L. Yarnell, G. P. Arnold, P. J. Bendt, E. C. Kerr, Phys. Rev. **113**, 1379 (1959).

[22] R.A. Cowley and A.D.B. Woods, Can. J. Phys. **49**, 177 (1971); A.D.B.Woods, R.A. Cowley, Rep Prog Phys **36** 1135 (1973).

[23] O.W. Dietrich, E. H. Graf, C. H. Huang, and L. Passell, Phys. Rev. A **5**, 1377 (1972).

[24] E.H. Graf, V.J. Minkiewicz, H. Bjerrum Moller, L. Passell, Phys. Rev. A **10**, 1748 (1974).

[25] H.R. Glyde and T. Griffin, Phys. Rev. Lett. **65**, 1454 (1990).

[26] B. Fåk and K.H. Andersen, Phys. Lett. A **160**, 468 (1991).

[27] F. Pistolesi, Phys. Rev. Lett. **81**, 397 (1998); F. Pistolesi, J. Low Temp. Phys. **113**, 597 (1998).

[28] B. Fåk, T. Keller, M. E. Zhitomirsky and A. L. Chernyshev, Phys. Rev. Lett. **109**, 155305 (2012).

[29] Y. Castin, A. Sinatra and H. Kurkijan, Phys. Rev. Lett. **119**, 260402 (2017).

[30] K. Beauvois, H. Godfrin, E. Krotscheck, and R. Zillich, J. Low Temp. Phys. **197**, 113 (2019).

[31] H.R. Glyde, M. R. Gibbs, W. G. Stirling, and M. A. Adams, Europhys. Lett. **43**, 422 (1998).

[32] J. V. Pearce, R.T. Azuah, B. Fåk, A R Sakhel, H. R Glyde and W. G. Stirling, J. Phys. Condens. Matter **13**, 4421 (2001).

[33] J. V. Pearce, R.T. Azuah, W. G. Stirling, R.M. Dimeo, P.S. Sokol, M.A. Adams, J. Low Temp. Phys. **124**, 573 (2001).

[34] B. Fåk and J. Bossy, J. Low Temp. Phys. **112**, 1 (1998).

[35] B. Fåk and J. Bossy, J. Low Temp. Phys. **113**, 531 (1998).

[36] K. H. Andersen, W. G. Stirling, R. Scherm, A. Stunault, B. Fåk, H. Godfrin, and A. J. Dianoux, J. Phys. Condens. Matter **6**, 821 (1994).

[37] K. H. Andersen, J. Bossy, J. C. Cook, O. G. Randl, and J.-L. Ragazzoni, Phys. Rev. Lett. bf 77, 4043 (1996).

[38] H.R. Glyde, J. Phys. Condens. Matter **32**, 374002 (2020).

[39] W. Götze , M. Lücke, Phys Rev B **13** 3825 (1976).

[40] K. Beauvois, J. Dawidowski, B. Fåk, H. Godfrin, E. Krotscheck, J. Ollivier, and A. Sultan, Phys. Rev. B **97**, 184520 (2018).

[41] K. Beauvois, C. E. Campbell, J. Dawidowski, B. Fåk, H. Godfrin, E. Krotscheck, H.-J. Lauter, T. Lichtenegger, J. Ollivier and A. Sultan, Phys. Rev. B **94**, 024504 (2016).

[42] W. Montfrooij, E.C. Svensson, Physica B **241-243** 924 (1997).

[43] M.R. Gibbs, W.G. Stirling, J. Low Temp. Phys. **102**, 249 (1996).

[44] M.R. Gibbs, W. G. Stirling, K. H. Andersen, R. Azuah, H. Schober, J. Dianoux, J. Phys. Cond. Matter **8**, 9417 (1996).

[45] M.R. Gibbs, K. H. Andersen, W. G. Stirling and H. Schober, J. Phys. Cond. Matter **11**, 603 (1999).

[46] M.R. Gibbs, W. G. Stirling, K. H. Andersen, H. Schober, J. Low Temp. Phys. **120**, 55 (2000).

[47] G. Zsigmond, F. Mezei, C.J. Carlile, Physica B **234-236** 327 (1997).

[48] H. Godfrin, K. Beauvois, A. Sultan, E. Krotscheck, J. Dawidowski, B. Fåk, and J. Ollivier Phys. Rev. B 103, 104516 (2021)

[49] Proposal number: RB14921

[50] O. Kirichek et al., J. Phys.: Conf. Ser. **150**, 012022 (2009).

[51] M.T.F. Telling and K.H. Andersen, Phys Chem Chem Phys **7**, 1255 (2005).

[52] F. Demmel and K. Pokhilchuk, Nucl. Instr. and Meth. A **767**, 426 (2014).

[53] O. Arnold, J.C. Bilheux, J.M. Borreguero, A. Buts, S.I. Campbell, L. Chapon, M. Doucet, N. Draper, R. Ferraz Leal, M.A. Gigg, V.E. Lynch, A. Markvardsen, D.J. Mikkelson, R.L. Mikkelson, R. Miller et al., Nucl Instr and Meth A **764**, 156 (2014).